


Thermally induced diphenylalanine cyclization in solid phase

Marat A. Ziganshin¹  · Alexander V. Gerasimov¹ · Sufia A. Ziganshina^{1,2} ·
Nadezhda S. Gubina¹ · Guzel R. Abdullina¹ · Alexander E. Klimovitskii¹ ·
Valery V. Gorbachuk¹ · Anastas A. Bukharaev²

Received: 4 December 2015 / Accepted: 7 April 2016
© Akadémiai Kiadó, Budapest, Hungary 2016

Abstract The reaction of cyclization of diphenylalanine in solid phase under heating was studied, which is a stage in formation of various nanostructures from this dipeptide. The temperature ranges of the reaction as well as of dehydration of clathrate of diphenylalanine with water were determined. Kinetic parameters of cyclization were estimated within the approaches of the non-isothermal kinetics (“model-free” kinetics and linear regression methods for detection of topochemical equation). The product of diphenylalanine cyclization was characterized by X-ray powder diffractometry, FTIR spectroscopy and TG/DSC analysis. Crystallization of diphenylalanine and cyclo(diphenylalanine) from methanol solutions was studied using atomic force microscopy. The results obtained may be useful for the design of new nanomaterials based on diphenylalanine at high temperatures.

Keywords Diphenylalanine · Reaction of cyclization · Thermal analysis · Nanostructures · X-ray powder diffraction · Atomic force microscopy

Introduction

The interest to materials based on short-chain oligopeptides is caused by their unique properties and potential advantages for various technologies [1–3]. A feature of such oligopeptides is their ability to self-organize with formation of various nanostructures: nanospheres, nanorods, nanotubes, nanovesicles, etc. [4]. Crystals based on dipeptides have the porosity and demonstrate the zeolite-like properties [5, 6] being capable of selective binding of some gases: CO₂, CH₄, H₂ and Xe [7, 8]. Oligopeptide materials are used as templates for formation of metal nanowires [9] and as cathodes in Li-ion batteries based on peptide/Co₃O₄ composite nanowires [10], for fabrication of high-performance sensors [11]. Herewith, such materials have very low toxicity and constitute environmental alternatives to inorganic materials or MOFs [12].

To date, one of the most studied dipeptides, for which a large number of different nanostructures were synthesized, is diphenylalanine (**FF**) [13, 14]. Also its cyclic analog cyclo(diphenylalanine) (**cFF**) is actively studied. Previously, these dipeptides were used as bioligands in organometallic complexes [15]. For **cFF** the anthelmintic activity was found, which allows to use it as a drug [16]. But, the real boom in investigations of these oligopeptides was due to the discovery of the possibility to control the organization of their molecules to produce new nanomaterials. Magnetic field [17], relative humidity in the growth chamber and concentration of dipeptide [18], the type of solvent, from which dipeptide was crystallized [19, 20], were found to have an effect on their self-organization.

However, the most common method for formation of nanostructures based on diphenylalanine is the thermal treatment of its powder or amorphous film under different atmospheres: vacuum, inert gas, organic vapors or water

✉ Marat A. Ziganshin
Marat.Ziganshin@kpfu.ru

¹ A. M. Butlerov Institute of Chemistry, Kazan Federal University, Kremlevskaya, 18, Kazan, Russia 420008

² Kazan Zavoisky Physical-Technical Institute of the Kazan Scientific Center of the Russian Academy of Sciences, Sibirskii Trakt, 10/7, Kazan, Russia 420029

vapors [13, 21]. As a result, there is sublimation of dipeptide powder with subsequent condensation of nanostructures on cold surfaces or formation of nanostructures on the surface of initially amorphous film.

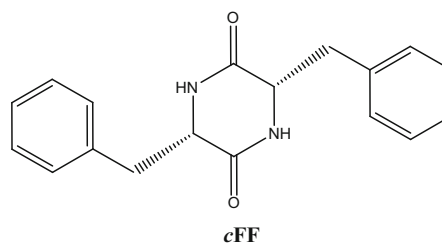
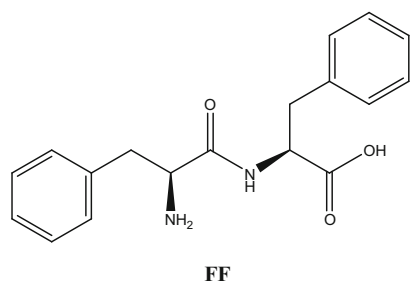
Studies of the temperature effect on diphenylalanine allowed to establish that during the heating up to 100 °C, **FF** loses water, while **cFF** do not lose the mass up to 250 °C [21]. After the sublimation of **FF** at 230 °C in argon, this dipeptide is condensed on the surface of the silicon substrate at 180 °C with formation of **cFF** nanowires [21]. The formation of **cFF** nanotubes also occurs after the **FF** sublimation under vacuum at 220 °C and subsequent condensation on the substrate surface at 80 °C [22]. On the other hand, nanotubes based on **FF** remain unchanged up to 150 °C. A significant structural destruction did occur when the nanotubes were heated to 200–300 °C. At temperatures above 50 °C, the nanotubes lose 15 mass% of their mass, which the authors attributed

differential scanning calorimetry (DSC) and mass spectrometric (MS) detection of evolved vapors at different heating rates. The kinetic parameters of the reaction were determined. The initial sample of **FF** and the product of its heating were characterized by a number of different methods: X-ray powder diffraction (XRPD), Fourier transform infrared spectroscopy (FTIR) and atomic force microscopy (AFM). Obtained results were compared with the results of commercially available **cFF**.

Experimental

Materials

Dipeptides diphenylalanine (**FF**) (Chem-Impex, Cat#06181) and cyclo(diphenylalanine) (**cFF**) (Chem-Impex, Cat#11058) were used without additional purification.



to desorption of water [23]. If the amorphous film of **FF** is heated in contact with aniline vapors up to 150 °C, the peptide nanowires (PNWs) are formed, but in the atmosphere of water vapors at 25 °C the peptide nanotubes (PNTs) are formed. PNTs started to lose their structural integrity even at 100 °C and were fully fragmented at 200 °C; PNWs maintained their initial structure even at 200 °C. Furthermore, in the case of PNWs, there is no thermal decomposition of peptide building blocks before 308 °C [24]. It should be noted that in these studies the thermal PNWs behavior is very similar to that of **cFF**.

Thus, in formation of nanostructures based on **FF** by heating, the possibility of diphenylalanine cyclization giving **cFF** should be considered. No such considerations were made in a number of studies where nanostructures were obtained from **FF** at high temperatures in solid phase [10, 25] and in solution [26]. Moreover, the temperature ranges and conditions for this reaction in powder under heating have not been established.

The present work is the first study of **FF** cyclization in the solid phase under heating. This reaction was studied using thermogravimetric (TG) analysis with simultaneous

The product of solid-state reaction of cyclization of diphenylalanine (**hFF**) was prepared by heating of **FF** up to 250 °C in argon atmosphere.

Thermoanalysis by simultaneous TG/DSC/MS

Simultaneous thermogravimetry (TG) and DSC analysis of dipeptide powder with mass spectrometric (MS) evolved gas analysis were performed using thermoanalyzer STA 449 C Jupiter (Netzsch) coupled with quadrupolar mass spectrometer QMS 403C Aeolos (Netzsch) as described elsewhere [27, 28]. For experiments, 7–12 mg samples of dipeptide were placed in aluminum crucibles (40 μ L) with lids having 3 holes, each of 0.5 mm in diameter.

Kinetic analysis of reaction of diphenylalanine cyclization in solid phase

According to ICTAC recommendations, it is necessary to use at least two different kinetic computational methods [29, 30]. The “model-free” methods for kinetic computations: Ozawa-Flynn-Wall, ASTM E698 and Friedman

[31–35] were used. The same set of experimental data was used further for searching the topochemical equation as described in [36–39]. The data for kinetic analysis were obtained from TG data, measured at different heating rates: 2, 5, 10 and 15 K min⁻¹. Calculations were performed using NETZSCH Thermokinetics 3.1.

Powder X-ray diffraction

X-ray powder diffraction (XRPD) studies of dipeptides were made using a MiniFlex 600 diffractometer (Rigaku) equipped with a D/teX Ultra detector. In this experiment, Cu K α radiation (40 kV, 15 mA) was used and data were collected at room temperature in the range of 2θ from 3 to 50 with a step of 0.02 and exposure time at each point of 0.24 s without sample rotation.

Fourier transform infrared spectroscopy analysis

FTIR spectra were collected using Bruker Vertex 70 FTIR spectrometer with a single reflection, germanium crystal ATR accessory (MIRacle, PIKE Technologies) with resolution of 2 cm⁻¹ in dry air. All data were collected at 25 °C.

Atomic force microscopy (AFM)

AFM images were recorded using the atomic force microscopes Solver P47Pro and Titanium (NT-MDT, Russia). Measurements were performed on air using a tapping mode [40]. Single silicon cantilevers NSG-11 or revolution cartridge of cantilevers (NT-MDT, Russia) were used. For AFM experiments, dipeptide films with diameter of 3 mm were prepared on the surfaces of highly oriented pyrolytic graphite (HOPG) plates (1 × 1 cm) [28]. HOPG was freshly cleaved before use.

Results and discussion

Thermal analysis

The samples of diphenylalanine (**FF**), cyclo(diphenylalanine) (**cFF**) and product of solid-state cyclization of diphenylalanine (**hFF**) were studied by TG/DSC/MS analysis, Fig. 1.

The TG curve obtained for **FF** powder contains at least four steps of decomposition, which corresponds to the very complex shape of DSC curve with multiple peaks, Fig. 1a. The first step ends at 127 °C, second at 147 °C, third at 185 °C and the fourth at 250 °C. At corresponding stages, the mass loss Δm is equal to 7.51, 1.60, 4.90 and 1.44 %.

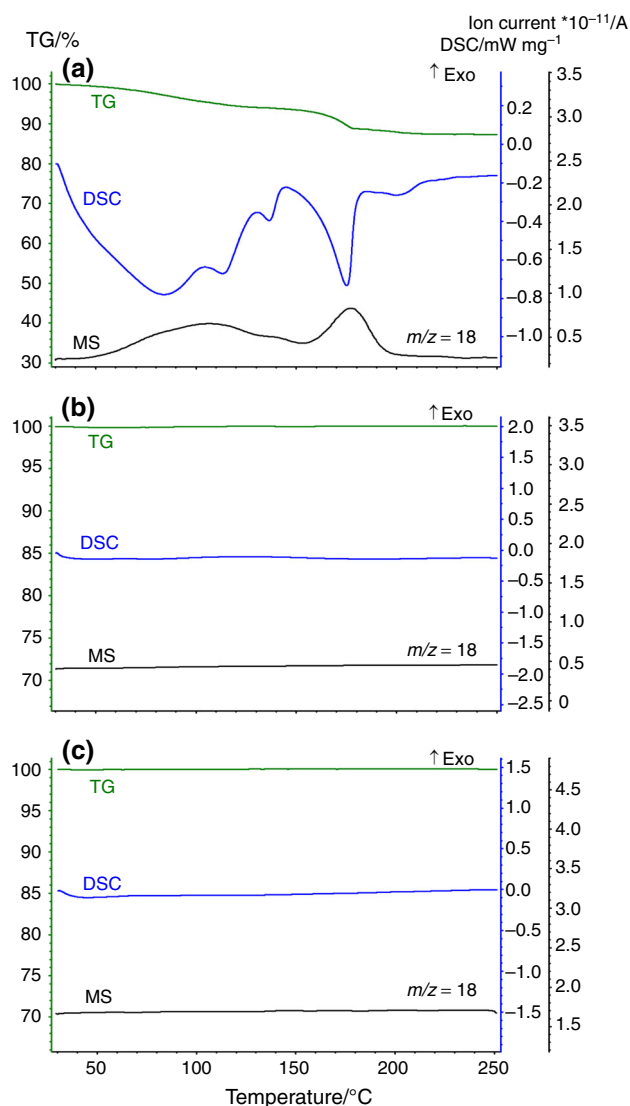


Fig. 1 The data of TG/DSC/MS analysis for powder of **a FF**, **b cFF** and **c hFF**. MS curve of evolved H₂O ($m/z = 18$) is shown. Heating rate is 10 K min⁻¹

According to MS data, the water vapor ($m/z = 18$) evolves at all these stages, except the fourth step of mass loss.

The total mass loss of the **FF** sample during the heating up to 250 °C is $\Delta m = 15.45$ %. Water evolves up to 200 °C, while the corresponding process ends in the third step at 185 °C. The mass loss of the sample above 185 °C ($\Delta m = 1.44$ %) without corresponding MS signal of water may be related to the partial decomposition of dipeptide. Thus, the mass loss associated with the elimination of water ($\Delta m = 14.01$ %) corresponds to the ratio 2.8 mol of water per 1 mol of dipeptide.

According to the reaction equation, **FF** cyclization gives one molecule H₂O. So we have assumed that the initial sample of **FF** represents the clathrate **FF**·1.8H₂O and the

reaction of cyclization occurs at temperatures above 147 °C at the third stage of the mass loss, where the elimination of water is in the relatively narrow temperature range.

The results of thermal analysis of **cFF** and **hFF** show that these dipeptides are stable up to 250 °C, because there is no mass loss and there are no signals on the DSC curves, Fig. 1b, c. The high thermal stability of **cFF** and **hFF** is in good agreement with literature data. According to that data, each molecule of dipeptide in the solvent-free crystals of cyclo(diphenylalanine) prepared by sublimation under reduced pressure [41] forms, in average, a pair of hydrogen bonds $\text{NH}\cdots\text{O}$ [42] and participates in van der Waals interactions [43]. Such features can provide the increase in mechanical and thermal stability of crystals.

X-ray powder diffraction study

The powders of dipeptides were characterized by XRPD method, Fig. 2. The data obtained show the significant differences in the packing of **FF**, Fig. 2a, and its cyclic analog **cFF**, Fig. 2b, and **hFF**, Fig. 2c.

The positions of the main peaks in the diffractogram of **hFF**, Fig. 2c, are identical to those of **cFF** diffractogram,

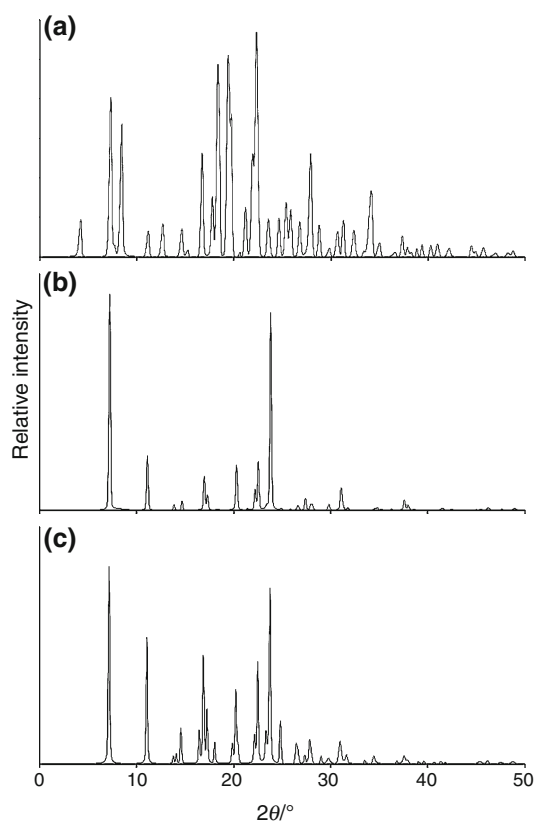


Fig. 2 X-ray powder diffractograms of **a FF**, **b cFF** and **c hFF**

Fig. 2b. But the former one contains several peaks at 2θ angles equal to 16.4°, 18.0° and 19.8° (with an intensity of about 20 % from the most intense peak at $2\theta = 7.2^\circ$), which are practically absent on the diffractogram of **cFF** (<1.3 % the intensity from the most intense peaks at $2\theta = 7.2^\circ$). It should be noted that the diffraction patterns of **FF** and **hFF**, obtained in the present study, are in good agreement with the diffractograms simulated from X-ray monocrystal data [41, 44]. Interestingly, for the nanostructures obtained by heating of **FF** with aniline vapor, there are peaks at 2θ equal to 6.8° and 20.5° on the diffractogram [25]. The rather close peaks ($2\theta = 7.18^\circ$ and 20.2°) are on the diffractogram of **hFF**, while on the diffractogram of **FF** such peaks are absent. So, one cannot exclude the formation of **cFF** after heating of dipeptide **FF** with pyridine vapor.

Data of Fourier transform infrared spectroscopy

FTIR spectra obtained for the powders of **FF**, **cFF** and **hFF** are presented in Fig. 3.

FTIR spectra of **cFF**, Fig. 3b, and **hFF**, Fig. 3c, are identical and differ from the spectrum of **FF**, Fig. 3a. For the latter, the band of $-\text{NH}_2$ and $-\text{OH}$ groups has enlarged shoulder at 3550 cm^{-1} , which may be caused by the

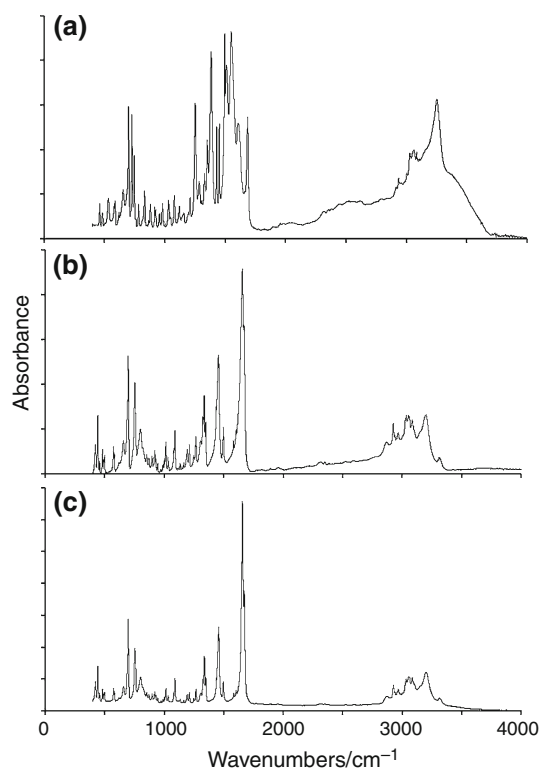


Fig. 3 FTIR spectra of powders of **a FF**, **b cFF** and **c hFF**

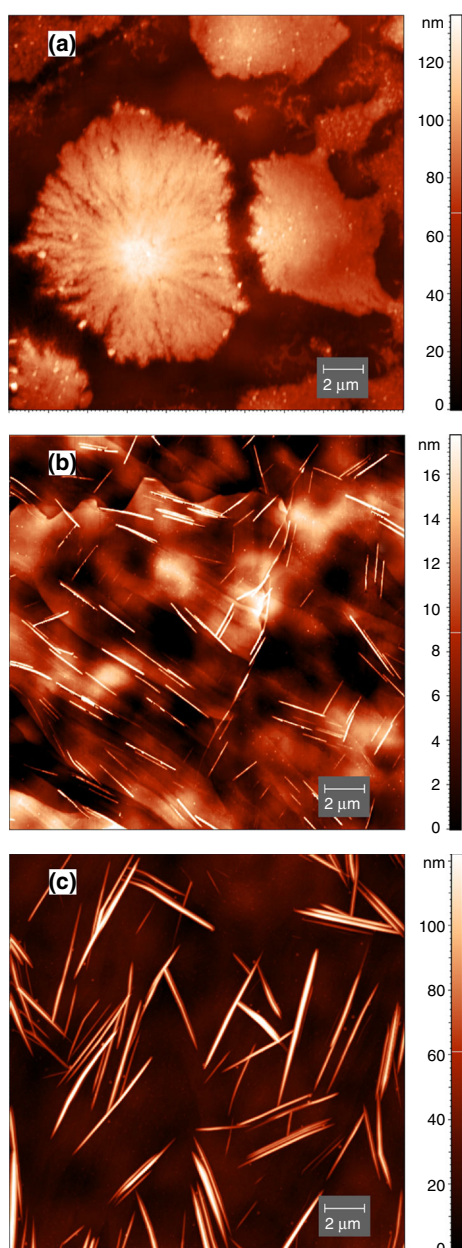


Fig. 4 AFM images of the surface of the **a** **FF**, **b** **cFF** and **c** **hFF** films deposited on the HOPG surface, $T = 298$ K. Before AFM experiment, all films were dried by hot air (45 °C) for 2 min

presence of water in the **FF** powder. The absence of explicit signals at 2500 , 1600 and 1500 cm^{-1} in the spectra of **cFF** and **hFF** confirms the absence of the free ammonium groups that are present in the crystals of **FF** [44].

AFM study of surface morphology

In the present work, the AFM images of the films of **FF**, **cFF** and **hFF** deposited from the methanol solution on the surface of the HOPG were obtained, Fig. 4. We have found that the **FF** forms large dendritic crystals with an average

diameter from 4 to 15 μm , Fig. 4a. The height of the crystals is 50 – 110 nm in the center and 35 – 80 nm at the borders.

For the **cFF**, the formation of nanorods with length of 1.2 – 4.0 μm , width of 150 – 280 nm and a height of 7 – 20 nm was observed, Fig. 4b. The similar structures were found after the crystallization of **hFF**, Fig. 4c. In the last case, the length, width and height of the nanorods were 2.3 – 8.2 μm , 200 – 520 and 30 – 120 nm, correspondingly. A specific feature of **hFF** structures is their narrower ends.

So, these studies prove the formation of cyclo(diphenylalanine) during the heating of powder of diphenylalanine up to 250 °C.

Kinetic analysis

To study the reaction of **FF** cyclization in the solid phase, it is necessary to correctly determine the temperature range of this process. The difficulty is in the fact that, according to X-ray monocrystal data [44] and our thermal analysis, this dipeptide contains the bound water. To solve this problem, three different samples of **FF** were prepared. The first sample **FF**₁ was heated up to 130 °C. At this temperature, we assume the absence of chemical reaction. The second one **FF**₂ was heated up to 147 °C, which corresponds to the end of the DTG peak. Above this temperature, a third step of the mass loss associated with the cyclization begins, Fig. 1a. The third sample **FF**₃ was heated up to the temperature 165 °C at which the reaction of cyclization must end. All samples were heated with rate of 10 K min^{-1} in the thermal analyzer as described in the experimental part. After reaching the target temperature, the samples were kept in isothermal conditions for 10 min, and then, they were cooled to room temperature.

The powders of these samples were characterized by XRPD, Fig. 5. The diffractogram of **FF**₃ completely coincides with the diffractogram of **cFF** and **hFF**, Figs. 2b, c–5. The diffractogram of **FF**₁, Fig. 5, contains all peaks corresponding to the diffractogram of initial **FF**, Fig. 2a, but a new peak at the angle of $2\theta = 5^\circ$ appears. For the

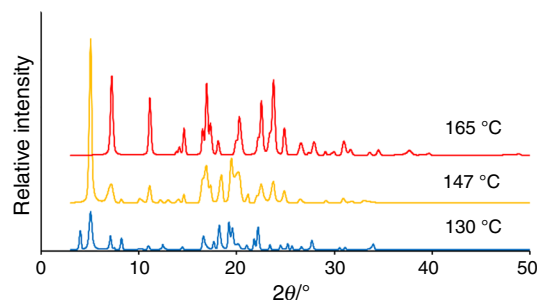


Fig. 5 X-ray powder diffractograms of dipeptide heated up to 130 °C (**FF**₁), 147 °C (**FF**₂), 165 °C (**FF**₃)

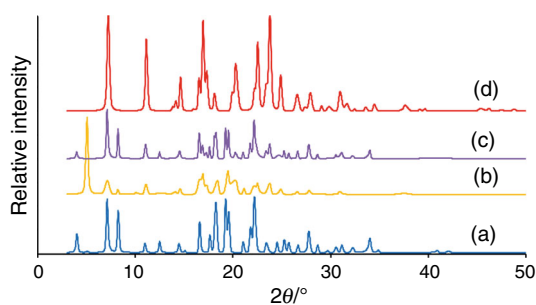


Fig. 6 X-ray powder diffractograms of **FF** heated up to different temperatures and saturated with water vapors of $P/P_0 = 1$ at 25 °C. The heating temperature/saturation time are *a* 130 °C/150 min, *b* 147 °C/3 h, *c* 147 °C/1 day, *d* 165 °C/3 days

sample of **FF**₂, the diffractogram obtained, Fig. 5, does not correspond neither to **FF**, Fig. 2a, nor to **cFF** (**hFF**), Fig. 2b, c. We assumed that the sample heated to 130 °C is a relatively stable intermediate hydrate formed by partial

dehydration of the initial **FF**·1.8H₂O clathrate, while only anhydrous **FF** is present at 147 °C.

To test this assumption, the samples obtained at different temperatures were saturated with vapors of water having thermodynamic activity of $P/P_0 = 1$ at 25 °C. We found that the **FF**₁ sample restores the crystal packing of **FF**·1.8H₂O clathrate in 150 min of equilibration with a saturated water vapor, Fig. 6a. The contact of **FF**₂ with this aqueous vapor for 3 h does not change the packing of dipeptide, Fig. 6b. But, after 24 h of saturation, the powder of **FF**₂ fully restores the initial packing of **FF**·1.8H₂O, Fig. 6c. The saturation of **FF**₃ with vapors of water even for 3 days does not change its diffractogram, Fig. 6d, which remains equivalent to diffractograms of **cFF** and **hFF**, Fig. 2b, c.

This study proves that the cyclization reaction of **FF** in powder form begins above 147 °C in the mentioned experimental conditions. Water eliminated above this temperature, Fig. 1a, is a reaction product. Therefore, the calculations of kinetic parameters of this reaction were

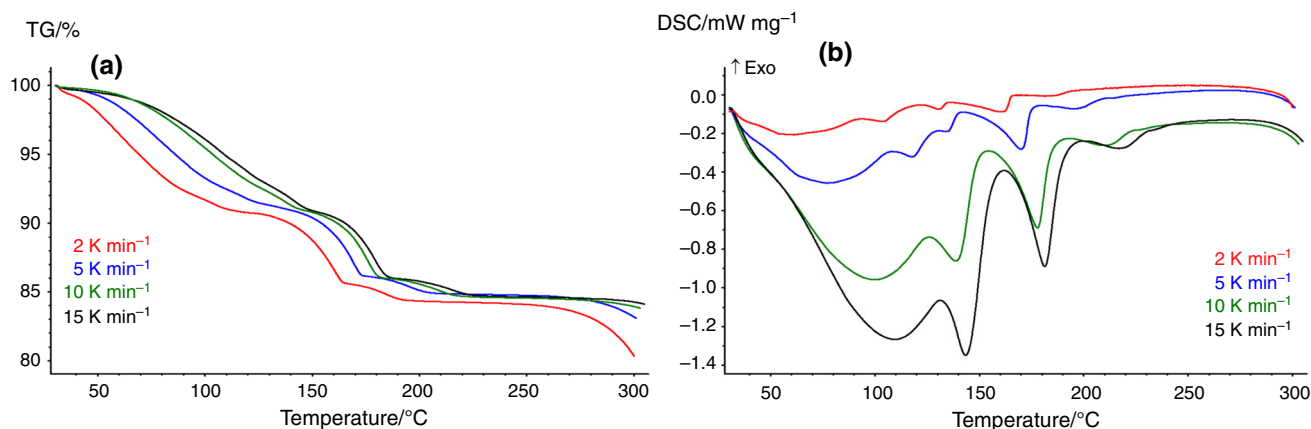


Fig. 7 The data of **a** TG and **b** DSC analysis for **FF** at different heating rates

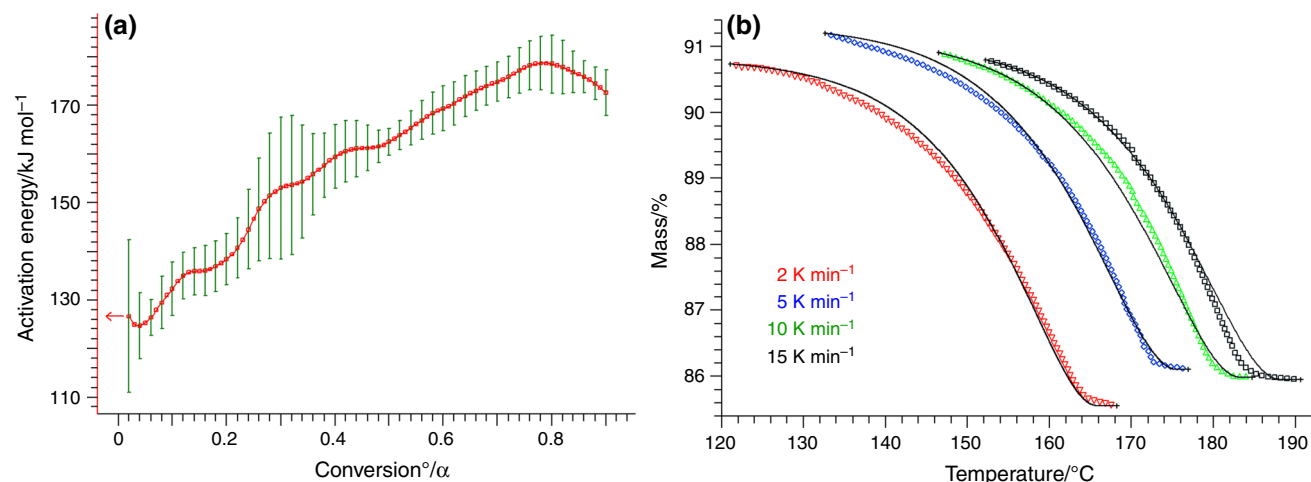


Fig. 8 Friedman analysis of reaction of **FF** cyclization: activation energies E_a versus degree of conversion α (**a**) and correlation of experimental points from TG curves with the calculated lines in accordance with equation R2 (**b**). Perpendicular lines show SD of calculation

Table 1 Kinetic parameters of the reaction $\mathbf{FF} \rightarrow \mathbf{hFF}$ and statistical parameters of calculation

Equation A \rightarrow B	F_{crit}	F_{exp}	F_{act}	$E_a/\text{kJ mol}^{-1}$	$\lg A$	Reaction order	Corr. coeff.
Fn	1.04	1.00	7726	148 ± 0.18	15.4 ± 0.02	0.46	0.997855
CnB	1.04	1.00	7725	148 ± 0.04	15.4 ± 0.004	0.46	0.997855
Bna	1.04	1.00	7725	148 ± 0.14	15.4 ± 0.01	0.46	0.997859
R2	1.04	1.02	7727	149 ± 0.05	15.2 ± 0.006	1/2	0.998025

The used topochemical equations are n th order (Fn), reaction with autocatalysis (CnB), Prout–Tompkins (Bna) and two-dimensional phase boundary reaction (R2) equations [45]. Data on the F test of fit quality (to identify the best kinetic description) [38]

made for the third step of mass loss, according to the TG curve showed in Fig. 1a.

The data for kinetic analysis were obtained from TG curves, Fig. 7, measured at different heating rates: 2, 5, 10 and 15 K min^{-1} .

Calculations of activation energies were made for selected temperature intervals: from 121.0 to 168.3 $^{\circ}\text{C}$ for heating rate of 2 K min^{-1} , from 132.7 to 177.0 $^{\circ}\text{C}$ for heating rate of 5 K min^{-1} , from 146.5 to 185.0 $^{\circ}\text{C}$ for heating rate of 10 K min^{-1} and from 152.2 to 190.7 $^{\circ}\text{C}$ for heating rate of 15 K min^{-1} .

According to Friedman method, the value of activation energy is $E_a = 162.5 \pm 2.7 \text{ kJ mol}^{-1}$ and logarithm of Arrhenius constant is $\lg A = 17.3$, whereas Ozawa–Flynn–Wall method gives $E_a = 140.6 \pm 4.5 \text{ kJ mol}^{-1}$ and $\lg A = 14.6$. The Friedman analysis of reaction of \mathbf{FF} cyclization is shown in Fig. 8a.

In accordance with F test, the best topochemical equations for the decomposition process are Fn, CnB, Bna or R2. The kinetic parameters calculated by using these models, as well as statistical quality parameters, are given in Table 1. The correlation of experimental points from TG curves with the calculated lines in accordance with equation R2 is shown in Fig. 8b.

The obtained values of activation energy, Arrhenius constant and reaction order are in good compliance with the calculated ones by Ozawa–Flynn–Wall approach. Thus, these kinetic parameters may be used to describe the reaction of cyclization of diphenylalanine in solid phase [46].

Conclusions

The solid-phase reaction of diphenylalanine cyclization was studied in the course of thermal analysis. The heating of the dipeptide powder leads to a two-stage decomposition accompanied with water evolution. Before the temperature 147 $^{\circ}\text{C}$, the desorption of water from $\mathbf{FF} \cdot 1.8\text{H}_2\text{O}$ occurs. Above 147 $^{\circ}\text{C}$, the reaction of diphenylalanine cyclization takes place. The formation of cyclo(diphenylalanine) was confirmed by the X-ray powder diffractometry and FTIR.

The calculated kinetic parameters of this reaction are $E_a = 148 \text{ kJ mol}^{-1}$, $A = 10^{15.4} \text{ s}^{-1}$, and the reaction order is 0.46.

The partially dehydrated clathrate of diphenylalanine having a crystal packing distinct from its dry form and saturated hydrate can be obtained by heating up to 130 $^{\circ}\text{C}$, while water-free diphenylalanine forms at 147 $^{\circ}\text{C}$. The partially or fully dried samples of diphenylalanine restore the initial packing of $\mathbf{FF} \cdot 1.8 \text{H}_2\text{O}$ by saturation with water. Herewith, for the water-free diphenylalanine, this process requires much more time than for the partially dried sample. Since the drying of diphenylalanine is an important part of the preparation of its amorphous film, our results may be used to control the degree of dipeptide dehydration or to prepare the water-free diphenylalanine.

The crystallization of diphenylalanine from the methanol solution on hydrophobic surface leads to formation of large dendritic crystals, while for cyclic dipeptide the nanorods were observed. In the latter case, the shape of 1D objects does not depend on the origin of the cyclo(diphenylalanine), but the size may vary. The results of present work can be useful for further development of techniques for preparation of nanomaterials based on oligopeptides.

Acknowledgements This study was supported by Russian Government Program of Competitive Growth of Kazan Federal University.

References

1. Busseron E, Ruff Y, Moulin E, Giuseppone N. Supramolecular self-assemblies as functional nanomaterials. *Nanoscale*. 2013;5: 7098–140.
2. Hamley IW. Peptide nanotubes. *Angew Chem Int Ed*. 2014;53:6866–81.
3. Ma H, Fei J, Li Q, Li J. Photo-induced reversible structural transition of cationic diphenylalanine peptide self-assembly. *Small*. 2015;11:1787–91.
4. Guo C, Luo Y, Zhou R, Wei G. Triphenylalanine peptides self-assemble into nanospheres and nanorods that are different from the nanovesicles and nanotubes formed by diphenylalanine peptides. *Nanoscale*. 2014;6:2800–11.

5. Afonso R, Mendes A, Gales L. Peptide-based solids: porosity and zeolitic behavior. *J Mater Chem*. 2012;22:1709–23.
6. Soldatov DV, Moudrakovski IL, Grachev EV, Ripmeester JA. Micropores in crystalline dipeptides as seen from the crystal structure, He pycnometry, and ^{129}Xe NMR spectroscopy. *J Am Chem Soc*. 2006;128:6737–44.
7. Comotti A, Bracco S, Distefano G, Sozzani P. Methane, carbon dioxide and hydrogen storage in nanoporous dipeptide-based materials. *Chem Commun*. 2009;3:284–6.
8. Soldatov DV, Moudrakovski IL, Ripmeester JA. Dipeptides as microporous materials. *Angew Chem Int Ed*. 2004;116:6468–71.
9. Reches M, Gazit E. Casting metal nanowires within discrete self-assembled peptide nanotubes. *Science*. 2003;300:625–7.
10. Ryu J, Kim S-W, Kang K, Park CB. Synthesis of diphenylalanine/cobalt oxide hybrid nanowires and their application to energy storage. *ACS Nano*. 2010;4:159–64.
11. Adler-Abramovich L, Badihi-Mossberg M, Gazit E, Rishpon J. Characterization of peptide-nanostructure-modified electrodes and their application for ultrasensitive environmental monitoring. *Small*. 2010;6:825–31.
12. Gorbitz CH. Microporous organic materials from hydrophobic dipeptides. *Chem Eur J*. 2007;13:1022–31.
13. Kim S, Kim JH, Lee JS, Park CB. Beta-sheet-forming, self-assembled peptide nanomaterials towards optical, energy, and healthcare applications. *Small*. 2015;11:3623–40.
14. Li Q, Ma H, Jia Y, Li J, Zhu B. Facile fabrication of diphenylalanine peptide hollow spheres using ultrasound-assisted emulsion templates. *Chem Commun*. 2015;51:7219–21.
15. Gleichmann AJ, Wolff JM, Sheldrick WS. η^5 -Pentamethylcyclopentadienylruthenium(II) complexes containing η^6 -co-ordinated dipeptides with aromatic side chains. *J Chem Soc Dalton Trans*. 1995;1:1549–54.
16. Walchshofer N, Sarciron ME, Garnier F, Delatour P, Petavy AF, Paris J. Anthelmintic activity of 3,6-dibenzyl-2,5-dioxopiperazine, cyclo(L-Phe-L-Phe). *Amino Acids*. 1997;12:41–7.
17. Hill RJA, Sedman VL, Allen S, Williams PM, Paoli M, Adler-Abramovich L, Gazit E, Eaves L, Tendler SJB. Alignment of aromatic peptide tubes in strong magnetic fields. *Adv Mater*. 2007;19:4474–9.
18. Wang M, Du L, Wu X, Xiong S, Chu PK. Charged diphenylalanine nanotubes and controlled hierarchical self-assembly. *ACS Nano*. 2011;5:4448–54.
19. Mason TO, Chirgadze DY, Levin A, Adler-Abramovich L, Gazit E, Knowles TPJ, Buell AK. Expanding the solvent chemical space for self-assembly of dipeptide nanostructures. *ACS Nano*. 2014;8:1243–53.
20. Li Q, Ma H, Wang A, Jia Y, Dai L, Li J. Self-assembly of cationic dipeptides forming rectangular microtubes and microrods with optical waveguiding properties. *Adv Opt Mater*. 2015;3:194–8.
21. Lee JS, Yoon I, Kim J, Ihee H, Kim B, Park CB. Self-assembly of semiconducting photoluminescent peptide nanowires in the vapor phase. *Angew Chem Int Ed*. 2011;50:1164–7.
22. Adler-Abramovich L, Aronov D, Beker P, Yevnin M, Stempler S, Buzhansky L, Rosenman G, Gazit E. Self-assembled arrays of peptide nanotubes by vapour deposition. *Nat Nanotechnol*. 2009;4:849–54.
23. Adler-Abramovich L, Reches M, Sedman VL, Allen S, Tendler SJB, Gazit E. Thermal and chemical stability of diphenylalanine peptide nanotubes: implications for nanotechnological applications. *Langmuir*. 2006;22:1313–20.
24. Ryu J, Park CB. High stability of self-assembled peptide nanowires against thermal, chemical, and proteolytic attacks. *Biotechnol Bioeng*. 2010;105:221–30.
25. Ryu J, Park CB. High-temperature self-assembly of peptides into vertically well-aligned nanowires by aniline vapor. *Adv Mater*. 2008;20:3754–8.
26. Huang R, Wang Y, Qi W, Su R, He Z. Temperature-induced reversible self-assembly of diphenylalanine peptide and the structural transition from organogel to crystalline nanowires. *Nanoscale Res Lett*. 2014;9:653–62.
27. Ziganshin MA, Gerasimov AV, Gorbachuk VV, Gubaidullin AT. Thermal analysis of clathrates of tripeptide LLL with organic compounds and water. *J Therm Anal Calorim*. 2015;119:1811–6.
28. Ziganshin MA, Gubina NS, Gerasimov AV, Gorbachuk VV, Ziganshina SA, Chuklanov AP, Bukharaev AA. Interaction of L-alanyl-L-valine and L-valyl-L-alanine with organic vapors: thermal stability of clathrates, sorption capacity and the change in the morphology of dipeptide films. *Phys Chem Chem Phys*. 2015;17:20168–77.
29. Vyazovkin S, Burnham AK, Criado JM, Luis A, Perez-Maqueda LA, Popescu C, Sbirrazzuoli N. ICTAC kinetics committee recommendations for performing kinetic computations on thermal analysis data. *Thermochim Acta*. 2011;520:1–19.
30. Vyazovkin S, Chrissafis K, Di Lorenzo M-R, Koga N, Pijolat M, Roduit B, Sbirrazzuoli N, Suñol J-J. ICTAC kinetics committee recommendations for collecting experimental thermal analysis data for kinetic computations. *Thermochim Acta*. 2014;590:1–23.
31. Kissinger HE. Variation of peak temperature with heating rate in differential thermal analysis. *J Res Natl Bur Stand*. 1956;57:217–21.
32. Friedman HL. Kinetics of thermal degradation of charforming plastics from thermogravimetry. Application to a phenolic plastic. *J Polym Sci*. 1964;6:183–95.
33. Ozawa T. A new method of analyzing thermogravimetric data. *Bull Chem Soc Jpn*. 1965;38:1881–6.
34. Ozawa T. Estimation of activation energy by isoconversion methods. *Thermochim Acta*. 1992;203:159–65.
35. Flynn JH, Wall LA. General treatment of the thermogravimetry of polymers. *J Res Natl Bur Stand*. 1966;70:478–523.
36. Logvinenko V, Drebushchak V, Pinakov D, Chekhova G. Thermodynamic and kinetic stability of inclusion compounds under heating. *J Therm Anal Calorim*. 2007;90:23–30.
37. Logvinenko VA, Dybtsev DN, Bolotov VA, Fedin VP. Thermal decomposition of inclusion compounds on the base of the metal-organic framework [Zn₂(bdc)₂(dabco)]. *J Therm Anal Calorim*. 2015;121:491–7.
38. Logvinenko VA, Aliev SB, Fedin VP. Thermal (kinetic) stability of the inclusion compound on the base of Li-contain MOF [Li₂(H₂btc)]-dioxane. *J Therm Anal Calorim*. 2015;120:53–8.
39. Logvinenko V. Stability of supramolecular compounds under heating thermodynamic and kinetic aspects. *J Therm Anal Calorim*. 2010;101:577–83.
40. Ziganshin MA, Efimova IG, Gorbachuk VV, Ziganshina SA, Chuklanov AP, Bukharaev AA, Soldatov DV. Interaction of L-leucyl-L-leucyl-L-leucine thin film with water and organic vapors: receptor properties and related morphology. *J Pept Sci*. 2012;18:209–14.
41. Gdaniec M, Liberek B. Structure of cyclo(-L-phenylalanyl-L-phenylalanyl-). *Acta Cryst*. 1986;C42:1343–5.
42. Jeon J, Scott M. Shell self-assembly of cyclo-diphenylalanine peptides in vacuum. *J Phys Chem B*. 2014;118:6644–52.
43. Azuri I, Adler-Abramovich L, Gazit E, Hod O, Kronik L. Why are diphenylalanine-based peptide nanostructures so rigid? Insights from first principles calculations. *J Am Chem Soc*. 2014;136:963–9.
44. Gorbitz CH. Nanotube formation by hydrophobic dipeptides. *Chem Eur J*. 2001;7:5153–9.
45. Opfermann J. Kinetic analysis using multivariate non-linear regression. I. Basic concepts. *J Therm Anal Calorim*. 2000;60:641–58.
46. Logvinenko VA, Sapchenko SA, Fedin VP. Thermal decomposition of inclusion compounds on the base of the metal-organic framework [Zn₄(dmf)(ur)₂(ndc)₄]. Part I. *J Therm Anal Calorim*. 2014;117:747–53.